British Journal of Pharmacology

DOI:10.1111/bph.12436
www.brjpharmacol.org

RESEARCH PAPER

Riluzole activates TRPC5 channels independently of PLC activity

Julia M Richter, Michael Schaefer and Kerstin Hill

Rudolf-Boehm-Institute of Pharmacology and Toxicology, University of Leipzig, Leipzig, Germany

Correspondence
Kerstin Hill, Rudolf-Boehm-Institute of Pharmacology and Toxicology, University of Leipzig, Härtelstr. 16-18, 04107 Leipzig, Germany. E-mail: kerstin.hill@medizin.uni-leipzig.de

Keywords
riluzole; TRPC5; patch clamp electrophysiology; calcium imaging

Received
5 June 2013
Revised
5 September 2013
Accepted
15 September 2013

BACKGROUND AND PURPOSE

The transient receptor potential channel C5 (TRPC5) is a Ca^{2+}-permeable cation channel, which is predominantly expressed in the brain. TRPC5 is activated in a PLC-dependent manner by, as yet, unidentified endogenous messengers. Recently, modulators of TRPC5, like Ca^{2+}, pH and phospholipids, have been identified. However, the role of TRPC5 *in vivo* is only poorly understood. Novel specific modulators of TRPC5 might help to elucidate its function.

EXPERIMENTAL APPROACH

Novel modulators of TRPC5 were identified in a compound screening of approved drugs and natural compounds. The potency and selectivity of TRPC5-activating compounds were determined by fluorometric calcium imaging. The biophysical properties of channel activation by these compounds were analysed using electrophysiological measurements.

KEY RESULTS

Riluzole was identified as a novel activator of TRPC5 (EC_{50} 9.2 ± 0.5 μM) and its mechanism of action was shown to be independent of G protein signalling and PLC activity. Riluzole-induced TRPC5 currents were potentiated by La^{3+} and, utilizing TRPC5 mutants that lack La^{3+} binding sites, it was confirmed that riluzole and La^{3+} activate TRPC5 by different mechanisms. Recordings of excised inside-out patches revealed a relatively direct effect of riluzole on TRPC5.

CONCLUSIONS AND IMPLICATIONS

Riluzole can activate TRPC5 heterologously expressed in HEK293 cells as well as those endogenously expressed in the U-87 glioblastoma cell line. Riluzole does not activate any other member of the TRPC family and could, therefore, despite its action on other ion channels, be a useful pharmacological tool for identifying TRPC5-specific currents in immortalized cell lines or in acutely isolated primary cells.

Abbreviations

$[Ca^{2}+]_i$, intracellular free Ca^{2+} concentration; 2-APB, 2-aminoethoxydiphenyl borate; ALS, amyotrophic lateral sclerosis; HBS, HEPES-buffered solution; tet, tetracycline; TRPC5, transient receptor potential channel C5

Introduction

TRPC5 belongs to the canonical transient receptor potential channels (TRPC), which form non-selective calcium-permeable cation channels. Phylogenetic analysis revealed that TRPC proteins can be subdivided into three groups: TRPC1/C4/C5, TRPC3/C6/C7 and TRPC2. Within these subfamilies, the proteins can assemble as homotetramers or heterotetramers, generating ion channels with unique biophysical properties (Strubing *et al.*, 2001; Hofmann *et al.*, 2002). Heterologous co-expression studies of TRPC1 and TRPC5 demonstrate an altered current–voltage relationship and a distinct single channel conductance compared with homomeric TRPC5 currents. The interaction of TRPC1 and

TRPC5 was further confirmed by intermolecular FRET measurements in heterologous expression systems and by co-immunoprecipitations studies performed on isolated rat brains (Goel *et al.*, 2002; Hofmann *et al.*, 2002; Strubing *et al.*, 2003). TRPC5 is predominantly found in the CNS. *In situ* hybridization staining indicate its highest levels of expression in the hippocampus, olfactory bulb and in the amygdala (Lein *et al.*, 2007) (http://mouse.brain-map.org). Other tissues like gonads, heart, liver and vascular smooth muscle exhibit low expression levels of TRPC5 (Riccio *et al.*, 2002; Beech *et al.*, 2004; Fowler *et al.*, 2007). Recently, TRPC5 has been assigned a function in the regulation of the morphology and motility of neuronal growth cones and neurite length, as well as contributing to neurotransmitter release (Greka *et al.*, 2003; Munsch *et al.*, 2003; Hui *et al.*, 2006). Furthermore, TRPC5$^-$knockout mice exhibit diminished fear-related behaviour when confronted with innate aversive stimuli (Riccio *et al.*, 2009). The limited knowledge about the physiological function of TRPC5 is partially ascribable to the fact that there are, as yet, no known endogenous specific activators of TRPC5. Like all TRPC channels, TRPC5 can be indirectly activated by the stimulation of Gαq-linked receptors or growth factor receptors, which are coupled to PLC (Schaefer *et al.*, 2000; Putney, Jr, 2004). However, in contrast to TRPC3/C6/C7, TRPC5 is not directly gated by DAG, which is generated from phosphatidylinositol 4,5-bisphosphate (PIP_2) by PLC. Several diverse stimuli have been identified to modulate TRPC5 channel activity. Elevated intracellular calcium concentrations (Blair *et al.*, 2009), increased extracellular acidity (Semtner *et al.*, 2007) and phospholipids like PIP_2 (Otsuguro *et al.*, 2008) and lysophosphatidylcholine (which is assumed to distort the lipid bilayer) (Flemming *et al.*, 2006), have been reported to mediate TRPC5 activity. Moreover, metal ions like lead (Sukumar and Beech, 2010), and μM concentrations of trivalent lanthanides (La^{3+}, Gd^{3+}) can induce or augment TRPC5 currents (Jung *et al.*, 2003). Recently, genistein and rosiglitazone have also been shown to activate TRPC5 channels, independently of classical receptor activation (Wong *et al.*, 2010; Majeed *et al.*, 2011). To improve the understanding of the physiological relevance of TRPC5 and to address the channel pharmacologically, specific and potent modulators are required. In the present study, we identified and analysed riluzole [6-(trifluoromethoxy) benzothiazol-2-amine] as a novel TRPC5 activator. Riluzole is the only approved drug which delays the progression of amyotrophic lateral sclerosis (ALS) a motoneuron disease associated with an increased glutamate concentration (Lacomblez *et al.*, 1996; Schuster *et al.*, 2012). A number of recent studies have also proposed a clinical use for riluzole in psychiatric disorders due to its antidepressant properties (Pittenger *et al.*, 2008; Grant *et al.*, 2010). At the molecular level, riluzole has been shown to affect the activity of several ion channels. It is reported to block voltage-gated sodium channels (<1–10 μM) and to inhibit voltage-activated calcium channels (10–40 μM), thereby preventing repetitive neuronal firing and promoting neuronal survival (Huang *et al.*, 1997; Song *et al.*, 1997; Wang *et al.*, 2008). Riluzole also potentiates calcium-dependent potassium currents [2–20 μM; (Wu and Li, 1999)] and has been shown to activate $K_{2P}2.1$ (TREK1) and $K_{2P}4.1$ (TRAAK) channels (100 μM), two members of the 2-pore K^+ channels (Duprat *et al.*, 2000). For an extensive review of the effects of riluzole on ion channels, see Bellingham (2011). Here, we show that riluzole can also activate TRPC5 channels, heterologously expressed in HEK293 cells as well as endogenously expressed TRPC5 in the U-87 glioblastoma cell line. The activation mechanism was shown to be independent of cytosolic components like PLC activity or of intracellular calcium stores, indicating that riluzole has a rather direct effect on TRPC5.

Methods

Cell culture and reagents

The cDNA of murine TRPC5 was cloned into a pcDNA4/TO plasmid (Invitrogen Corporation, Carlsbad, CA, USA) and was stably transfected into the T-REx-HEK293 cell line (Invitrogen) to generate a tetracycline (tet)-regulated expression system of TRPC5 (T-REx$_{TRPC5}$). The cells were cultured in DMEM (PAA Laboratories, Pasching, Austria), containing 10% fetal calf serum, 2 mM L-glutamine, 100 units per mL penicillin, 0.1 mg·mL^{-1} streptomycin, 100 μg·mL^{-1} zeocin and 15 μg·mL^{-1} blasticidin (Invitrogen). TRPC5 expression was induced by 1 μg·mL^{-1} tet (Tet+, Sigma-Aldrich, St. Louis, MO, USA) for 48–72 h before measurements. Non-induced cells (Tet-) or T-REx parental cells were used as controls. HEK293 cell lines that stably express other TRP channels (YFP-tagged human TRPC3, YFP-tagged mouse TRPC4β, YFP-tagged human TRPC6, YFP-tagged mouse TRPC7, CFP-tagged rat TRPV1, YFP-tagged rat TRPV2, YFP-tagged rat TRPV3, YFP-tagged mouse TRPV4, CFP-tagged human TRPM8) were generated and maintained as described previously (Urban *et al.*, 2012). The generation of the HEK$_{TRPM3}$ cell line was described elsewhere (Fruhwald *et al.*, 2012). For transient transfections, pcDNA3 plasmids (Invitrogen) encoding YFP-tagged mouse TRPC5 and human TRPC1 were transfected into HEK293 cells with a jetPei transfection reagent according to the manufacturer's instructions (PEQLAB, Erlangen, Germany). In brief, cells were grown to 80% confluency in Earle's Minimum Essential Medium (MEM, PAA Laboratories) supplemented with 10% fetal calf serum, 2 mM L-glutamine, 100 U mL^{-1} penicillin, 0.1 mg·mL^{-1} streptomycin; 1–3 μg of plasmid was transfected with 6 μL jetPEI reagent. U-87 cells were cultured in Iscove's modified Dulbecco's Media (PAA Laboratories), containing 10% fetal calf serum, 2 mM L-glutamine, 100 U mL^{-1} penicillin and 0.1 mg·mL^{-1} streptomycin. All chemicals were purchased from Sigma Aldrich if not stated otherwise.

Small interfering RNA (siRNA)-mediated knock-down

Specific siRNA raised against human TRPC5 (si C5) was obtained from Dharmacon (Thermo Fisher Scientific, St. Leon-Rot, Germany). Sense strand: tga gtg gaa gtt tgc gag aa (Wu *et al.*, 2007). Scrambled siRNA (si sc, AllStars Negative Control siRNA) was used as a control and was purchased from Qiagen (Hilden, Germany). U-87 cells were seeded on 25 mm glass coverslips, coated with 25 μg·mL^{-1} poly-l-lysine (Sarstedt, Nümbrecht, Germany). Cells were transfected at a confluency of 60–80%; 100 pmol siRNA and 5 μL Lipofectamine 2000 were mixed in 500 μL Opti-MEM I (Invitrogen). The mixture was incubated for 20 min at room

temperature (RT) and then transferred into 1.5 mL antibiotic-free medium and applied to the cells. Six hours after transfection, the medium was replaced by fresh growth medium. Experiments were conducted after 72 h.

Confocal laser scanning microscopy

The subcellular distribution of YFP-tagged TRPC5 channels and of PKCε was visualized with a confocal laser scanning microscope (LSM510-META, 100×/1.46 Plan Apochromat, Carl Zeiss, Oberkochen, Germany). Cells were seeded onto glass coverslips as described previously, transferred into a bath chamber and mounted on the stage of an inverted microscope. Fluorescence was excited at 488 nm and emission was detected by using a bandpass filter of 505–550 nm wavelength. Differential interference contrast microscopy was performed to obtain transmitted-light images.

Fluorometric $[Ca^{2+}]_i$ imaging

For single-cell calcium measurements, cells were seeded onto glass coverslips at least 24 h before measurement, with a final confluency of about 60%. To induce TRPC5 expression, $T\text{-}REx_{TRPC5}$ cells were treated with 1 $\mu g \cdot mL^{-1}$ tet directly when seeded. Forty-eight to 72 h after this treatment, TRPC5 channel activity was measured. Cells were incubated for 30 min at 37°C with 2 µM fura-2/AM (Molecular Probes, Eugene, OR, USA) in a HEPES-buffered solution (HBS) containing (in mM): 134 NaCl, 6 KCl, 1 $MgCl_2$, 1 $CaCl_2$, 10 HEPES, pH 7.4. Coverslips were rinsed with HBS and transferred into a bath chamber of an inverted microscope (Axiovert 100, Carl Zeiss) operating with a monochromator-assisted (TILL-Photonics, Graefelfing, Germany) digital epifluorescence videomicroscope. Fura-2 was sequentially excited at 340, 358 and 380 nm. The emission was recorded through a long-pass filter with a 12-bit cooled CCD camera (IMAGO, TILL-Photonics). The calcium concentration was calculated as described previously (Lenz *et al.*, 2002).

To conduct the initial compound screen and to generate concentrations-response curves, cells were seeded into pigmented 384-well plates with a clear, flat bottom (15 000 cells per well, Corning, Tewksbury, MA, USA). TRPC5 expression was induced as described above. Cells were incubated for 30 min at 37°C with 4 µM fluo-4/AM (Invitrogen) dissolved in HBS. Fluorescence was recorded with a custom-made fluorescence plate-imaging device as described previously (Norenberg *et al.*, 2012). Fluorescence intensities were recorded and are expressed as F/F_0. In some experiments, cells were pretreated with thapsigargin (2 µM) to deplete $InsP_3$-sensitive Ca^{2+} stores. To induce TRPC5 channel activity, a mixture of agonists (Amix) was applied to stimulate GPCR that are endogenously expressed in HEK293 cells (Kawabata *et al.*, 1997; Schachter *et al.*, 1997; Zhu *et al.*, 1998); the Amix consisted of 300 µM ATP, 300 µM carbachol and 0.5 $U \cdot mL^{-1}$ thrombin. This mixture was used as the resulting calcium signals were stronger than those obtained after application of a single agonist (Amix 100%, ATP 45%, carbachol 61%, thrombin 64%). Furthermore, the agonist mixture minimized false positive results, which may be caused by GPCR-antagonistic compounds during the screening assay. The following compound libraries were used to conduct a medium-throughput compound screen: Spectrum Collection (MicroSource, Gaylordsville, CT, USA) and $LOPAC^{1280}$ (Sigma-Aldrich).

Electrophysiology

Patch clamp recordings were made in the whole-cell configuration or in excised inside-out patches. Channel activity was recorded using a Multiclamp 700B amplifier together with a digidata 1440A digitizer (Molecular Devices, Sunnyvale, CA, USA) controlled by the pCLAMP 10 software. Cells were seeded on glass coverslips and used for measurements at a density of 20–30%. All experiments were performed at room temperature. The extracellular solution for whole-cell recordings contained (in mM): 130 NaCl, 5 KCl, 1.2 $MgCl_2$, 1.5 $CaCl_2$, 8 glucose and 10 HEPES, pH 7.4 adjusted with NaOH. The standard pipette solution contained (in mM): 115 CsCl, 2 $MgCl_2$, 5 Na_2ATP, 0.1 Na GTP, 5.7 $CaCl_2$, 10 HEPES and 10 EGTA, pH 7.2 adjusted with CsOH, yielding a free calcium concentration of 200 nM using MaxChelator (http://maxchelator.stanford.edu). In some experiments, a modified pipette solution additionally contained 1 mM GDPβS. Voltage ramps from –100 to +100 mV (500 ms duration) were applied at 1 s intervals, filtered at 3 kHz (four-pole Bessel filter) and sampled at 5 kHz. For inside out recordings, the pipette solution contained (in mM): 140 NaCl, 5 CsCl, 2 $MgCl_2$, and 10 HEPES, pH 7.4 adjusted with NaOH. The bath solution contained (in mM): 140 CsCl, 4 Na_2ATP, 2 $MgCl_2$, 0.38 $CaCl_2$, 1 EGTA, 10 HEPES, pH 7.2, adjusted with CsOH. Free calcium concentration was calculated as 100 nM. Single channel currents were filtered at 3 kHz and sampled with 10 kHz. Patch pipettes were made from borosilicate glass with a resistance of 3–6 MΩ. Whole-cell series resistances were compensated by 70%. Compounds were applied by using a continuous gravity flow perfusion system and a recording chamber with a volume of 500 µL. In some experiments, cells were pre-incubated with the PLC inhibitor U73122 or its inactive analogue U73343 (5 µM, 3 min). After incubation, cells were washed with standard bath solution for 2 min before the patch clamp experiments (Thyagarajan *et al.*, 2009).

Data analysis

Ca^{2+} imaging (fluo-4) and electrophysiological data are presented as mean ± SEM. Each experimental approach consists of at least three independent experiments. The single-cell recordings (fura-2) shown are representative of multiple independent measurements. Single-cell traces are displayed as grey lines, the mean response is presented in black. Two sets of data were compared by Student's *t*-test using OriginPro8 (OriginLab Corporation, Northhampton, MA, USA) software. More than two sets of data were compared using one-way ANOVA followed by a Bonferroni *post hoc* test. $P < 0.05$ (*) was considered as being statistically significant. The half-maximal response (EC_{50}) was determined by fitting the data to Hill's equation using OriginPro8 software.

The drug/molecular target nomenclature conforms to *BJP's* Concise Guide to PHARMACOLOGY (Alexander *et al.*, 2013).

Results

Riluzole activates TRPC5 channels

To establish a reliable screening assay in a 384-well format, we first generated a tet-inducible HEK293 cell line, expressing

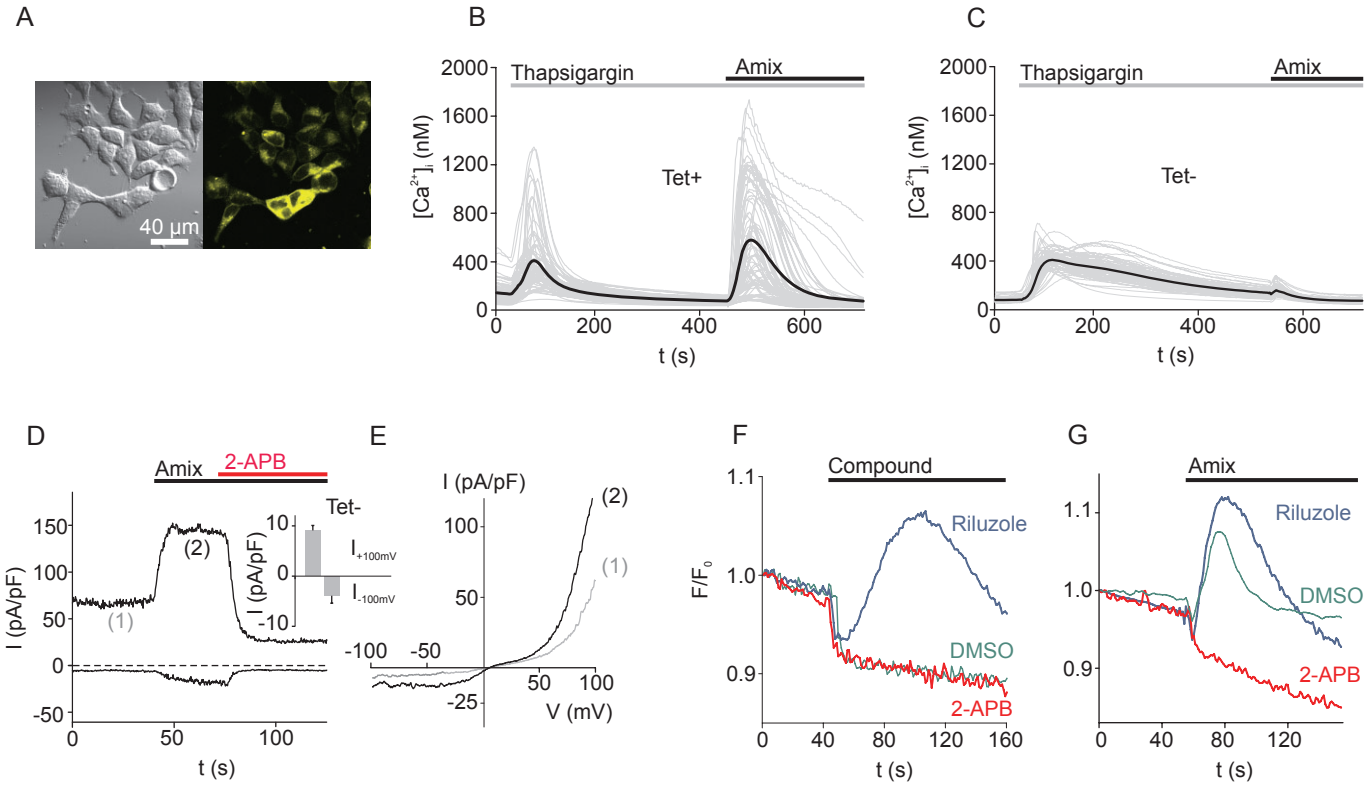

Figure 1

Receptor-mediated activation of TRPC5 in tet-inducible T-REx$_{TRPC5}$ cells. (A) Confocal imaging of HEK293-T-REx cells expressing YFP-tagged mTRPC5 after tet treatment (1 µg·mL^{-1} for 48 h; Tet+). (B, C) Fura-2-based single cell $[Ca^{2+}]_i$ measurements of induced (Tet+) and non-induced (Tet-) T-REx$_{TRPC5}$ cells. Thapsigargin (2 µM) was added to deplete InsP3-sensitive intracellular Ca^{2+} stores. TRPC5 channel activity was then stimulated by a mixture of agonists (Amix: 300 µM ATP, 300 µM carbachol, 0.5 U·mL^{-1} thrombin). (D) Representative whole-cell patch clamp recording of a Tet + T-REx$_{TRPC5}$ cell, upon stimulation with Amix and addition of 2-APB (75 µM). Data were extracted from voltage ramps and depict current amplitudes at +100 mV (upper trace) and –100 mV (lower trace). Inset: basal currents of non-induced T-REx$_{TRPC5}$ (Tet-) cells at +100 mV and –100 mV. Data represent means and SEM of four independent experiments. (E), I/V curves for basal (1) and Amix-induced (2) currents. (F, G) Exemplary calcium entry traces, obtained from a 384-well measurement. (F) Fluo-4-loaded cells were pretreated with thapsigargin (2 µM) 5 min before the compound (20 µM) was applied. Riluzole (blue trace) and 2-APB (red trace) are components of the Spectrum Collection. DMSO (green trace, 0.2%) served as control. (G) Amix was applied after 5 min to additionally identify compounds that block or sensitize TRPC5.

YFP-tagged TRPC5 (T-REx$_{TRPC5}$; Figure 1A). A mixture of GPCR agonists, consisting of ATP, carbachol and thrombin was used to stimulate TRPC5 channel activity. When cells were induced with tet, they responded with a strong Ca^{2+} signal in fura-2-based single-cell calcium imaging in contrast to tet-untreated cells, which were insensitive to the agonist mixture (Figure 1B, C). To exclude Ca^{2+} signals resulting from the depletion of intracellular calcium stores, cells were pretreated with thapsigargin (2 µM for 5 min). Patch clamp measurements also confirmed successful expression of TRPC5 channels. Tet-treated cells displayed a significant basal activity, as evident in Figure 1D and E compared with non-treated control cells (inset Figure 1D). Application of the agonist mixture further activated TRPC5-like currents in tet-treated cells (Figure 1D, E). Both, basal and agonist mixture-induced TRPC5 currents were sensitive to the unspecific TRPC5 channel blocker 2-aminoethoxydiphenyl borate (2-APB; Figure 1D).

In order to identify novel modulators of TRPC5 channel activity, we used the T-REx$_{TRPC5}$ cell line to conduct a 384-well-based medium-throughput screen. The primary screening data revealed that riluzole (blue trace, 20 µM), which is included in the Spectrum Collection as well as in the LOPAC^{1280} compound library, induced a robust Ca^{2+} signal in thapsigargin-pretreated T-REx$_{TRPC5}$ cells (Figure 1F). DMSO (green trace, 0.2%) and the unspecific TRPC5 channel blocker 2-APB (red trace, 20 µM; Xu *et al.*, 2005) were used as controls. The sudden decrease in the fluorescence signal after 50 s was caused by a dilution effect upon compound application. In order to identify further TRPC5-sensitizing or -blocking compounds, we additionally applied the agonist mix 5 min later (Figure 1G). The agonist mixture induced a robust Ca^{2+} response in cells pretreated with DMSO. The Ca^{2+} signal was even stronger when riluzole-pretreated cells were additionally stimulated with the agonist mixture. On the contrary, 2-APB-pretreated cells did not respond to the mixture of agonists (Figure 1G). The primary screening data was confirmed by fura-2-based single-cell $[Ca^{2+}]_i$ measurements. Riluzole induced long-lasting Ca^{2+} signals in tet-induced but not in non-induced T-REx$_{TRPC5}$ cells (Figure 2A, B). This activation

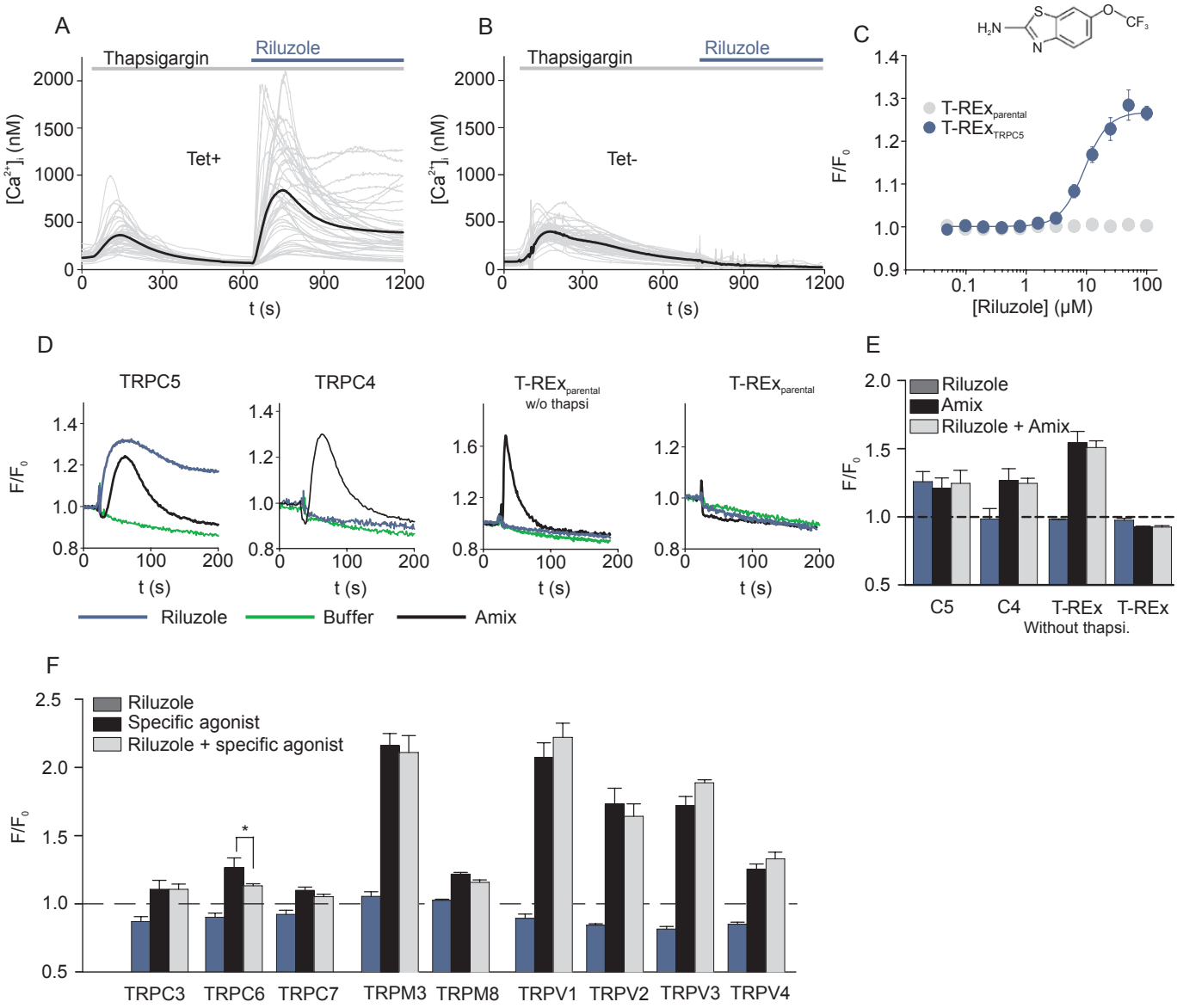

Figure 2

Riluzole elevates $[Ca^{2+}]_i$ in T-REx$_{TRPC5}$ cells independently of the filling state of intracellular Ca^{2+} stores. (A, B) Representative measurement of $[Ca^{2+}]_i$ in fura-2-loaded T-REx$_{TRPC5}$ cells with (Tet +; A) or without (Tet-; B) tet induction. Internal Ca^{2+} stores were depleted by thapsigargin treatment (2 μM) before riluzole (50 μM) was applied. (C) Concentration-response curves of riluzole for fluo-4-loaded T-REx$_{TRPC5}$ cells (Tet +; EC_{50} = 9.2 ± 0.5 μM) and parental cells (T-REx$_{parental}$). Data points represent means and SEM of 4–8 independent experiments. Inset: chemical structure of riluzole [6-(trifluoromethoxy) benzothiazol-2-amine]. (D) Representative examples of calcium entry traces of fluo-4-loaded T-REx$_{TRPC5}$ cells, TRPC4-expressing HEK293 cells and parental T-Rex cells after treatment with riluzole (50 μM, blue line), Amix (black line) or with HBS buffer (green line). Data were extracted from a 384-well measurement. All cells were pretreated with thapsigargin (2 μM, 5 min) before the measurements were obtained, except for T-REx$_{parental}$ (without thapsi.). (E) Statistical analysis of four independent experiments as in (D) after addition of riluzole (50 μM; blue bar), Amix (black bar) and riluzole together with Amix (grey bar). Dashed line indicates F/F_0 before compound addition. (F) Analyses of more distantly related TRP channels. Data presented are means and SEM of four independent experiments similar to the ones shown in (D). TRPC3- and TRPC6-expressing cells were pretreated with thapsigargin as described before. Cells were stimulated with riluzole (50 μM, blue bar), channel-specific agonists (black bar) or riluzole together with the channel-specific agonists (grey bar). Channel-specific agonists were as follows: Amix (TRPC3, C6); OAG (50 μM, TRPC7); PregS (30 μM, TRPM3); menthol (300 μM, TRPM8); capsaicin (2 μM, TRPV1); 2-APB (300 μM, TRPV2; 75 μM, TRPV3); GSK1016790A (100 nM, TRPV4). Dashed line indicates F/F_0 before compound addition.

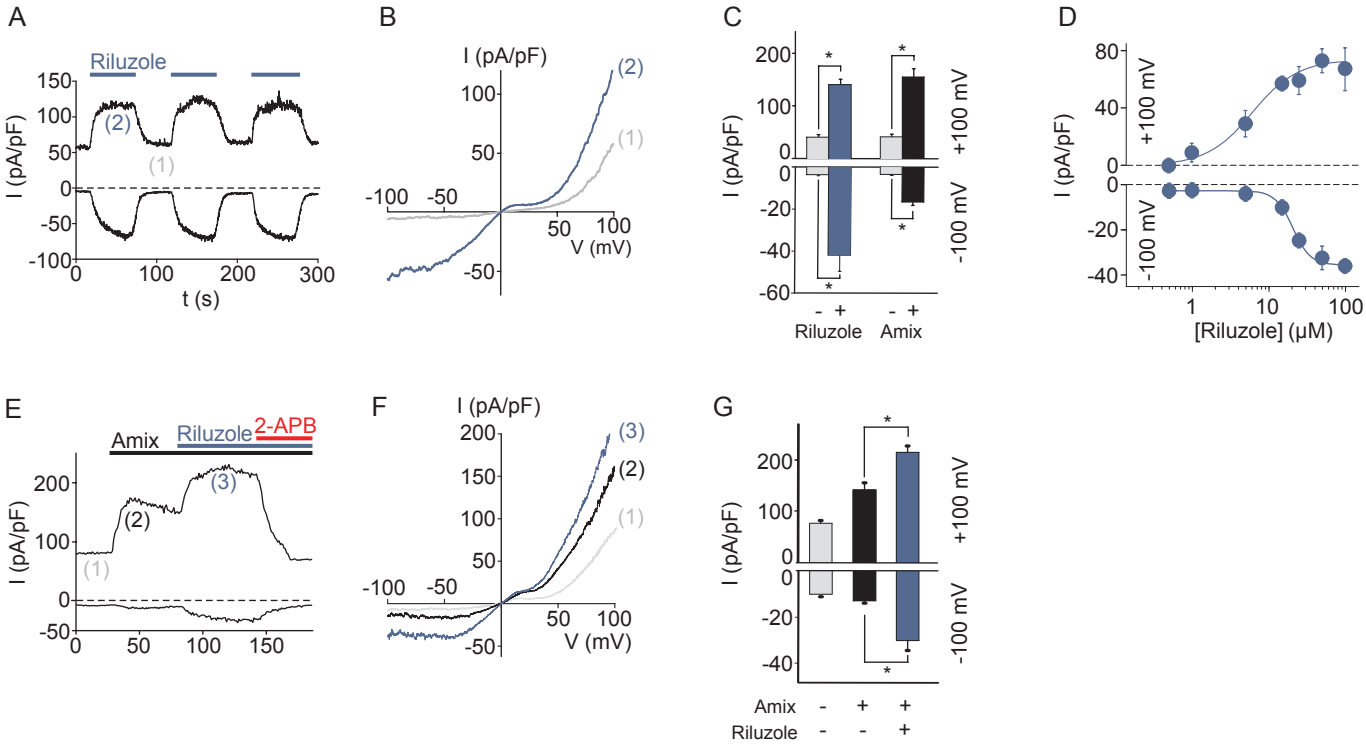

Figure 3

Reversible and repetitive stimulation of TRPC5 currents by riluzole. (A) Representative whole-cell recording, showing alternating applications and washout periods of riluzole (50 μM). Data were extracted from voltage ramps and depict current densities at +100 mV (upper trace) and –100 mV (lower trace). (B) I/V curves for basal (1) and riluzole-induced [50 μM; (2)] currents at the time points indicated in (A). (C) Statistical analysis of several independent experiments showing peak current densities before and after stimulation with riluzole (50 μM, $n = 8$) or Amix ($n = 3$; $^*P < 0.05$). (D) Concentration-response curve for riluzole-induced whole-cell currents at +100 mV (upper curve) and –100 mV (lower curve). $n > 3$ for each individual data point). (E) Whole-cell recording, demonstrating potentiation of Amix-induced TRPC5 currents by 10 μM riluzole and subsequent block by 2-APB (75 μM). Data were extracted from voltage ramps and depict current densities at +100 mV (upper trace) and –100 mV (lower trace). (F) I/V curves for basal (1), Amix-induced (2) and Amix- + riluzole-induced (3) currents. (G) Statistical evaluation of five independent experiments such as in (E); $^*P < 0.05$. Data represent means and SEM.

was independent of the filling state of the internal Ca^{2+} stores, which were depleted by thapsigargin prior to riluzole treatment or receptor activation. Measurements of concentration response curves revealed an EC_{50} of 9.2 ± 0.5 μM ($n \geq 4$ for each data point) for riluzole-induced TRPC5 activation (Figure 2C). Parental T-REx cells did not respond to riluzole (Figure 2C–E). We tested whether a panel of other TRP channels was also affected by riluzole, utilizing stably transfected HEK293 cell lines as established before (Urban *et al.*, 2012). TRPC4, the closest homolog to TRPC5, was not activated by 50 μM riluzole (Figure 2D, E). The same applied to TRPC3, TRPC6 and TRPC7, the vanilloid receptors-like channels (TRPV1, TRPV2, TRPV3, TRPV4) and the melastatin-related TRPM3 and TRPM8 channels (Figure 2F). Except for TRPC6, which was partially blocked by 50 μM riluzole, none of the TRP channels tested were inhibited by riluzole (Figure 2F).

In whole-cell patch clamp recordings, TRPC5 was reversibly activated by alternating stimulation and wash out periods of riluzole (Figure 3A). The resulting currents exhibited the typical characteristics of TRPC5 with its low conductance at low positive voltages and a reversal potential close to 0 mV (Figure 3B). Compared with the receptor-induced TRPC5 activation, the inward currents after riluzole stimulation were more pronounced (Figure 3C). The concentration response relationships for the riluzole-induced TRPC5 activation yielded EC_{50} values of 6.2 ± 1.1 μM at +100 mV and 20.7 ± 0.7 μM at –100 mV (Figure 3D). When cells were prestimulated with the mixture of agonists, 10 μM riluzole was sufficient to efficiently potentiate the TRPC5 inward current from –12.9 ± 0.8 pA/pF to –30.2 ± 4.5 pA/pF ($n = 5$, Figure 3E–G).

Riluzole activates TRPC5 independently of G protein and PLC signalling

We next wanted to know whether G protein signalling or PLC is involved in the riluzole-mediated TRPC5 activation. The stimulation of Gαq protein-coupled GPCRs via ATP, carbachol or thrombin leads to the activation of PLC, which in turn generates DAG that causes the translocation of the PKCε to the plasma membrane. We examined a possible involvement of PLC by utilizing a HEK293 cell line that stably expressed YFP-tagged PKCε [$HEK_{PKCε\text{-}YFP}$ (Schaefer *et al.*, 2001)] In untreated $HEK_{PKCε\text{-}YFP}$ cells, the YFP fluorescence was evenly distributed within the cytosol. The distribution did not change when cells were challenged with riluzole, indicating

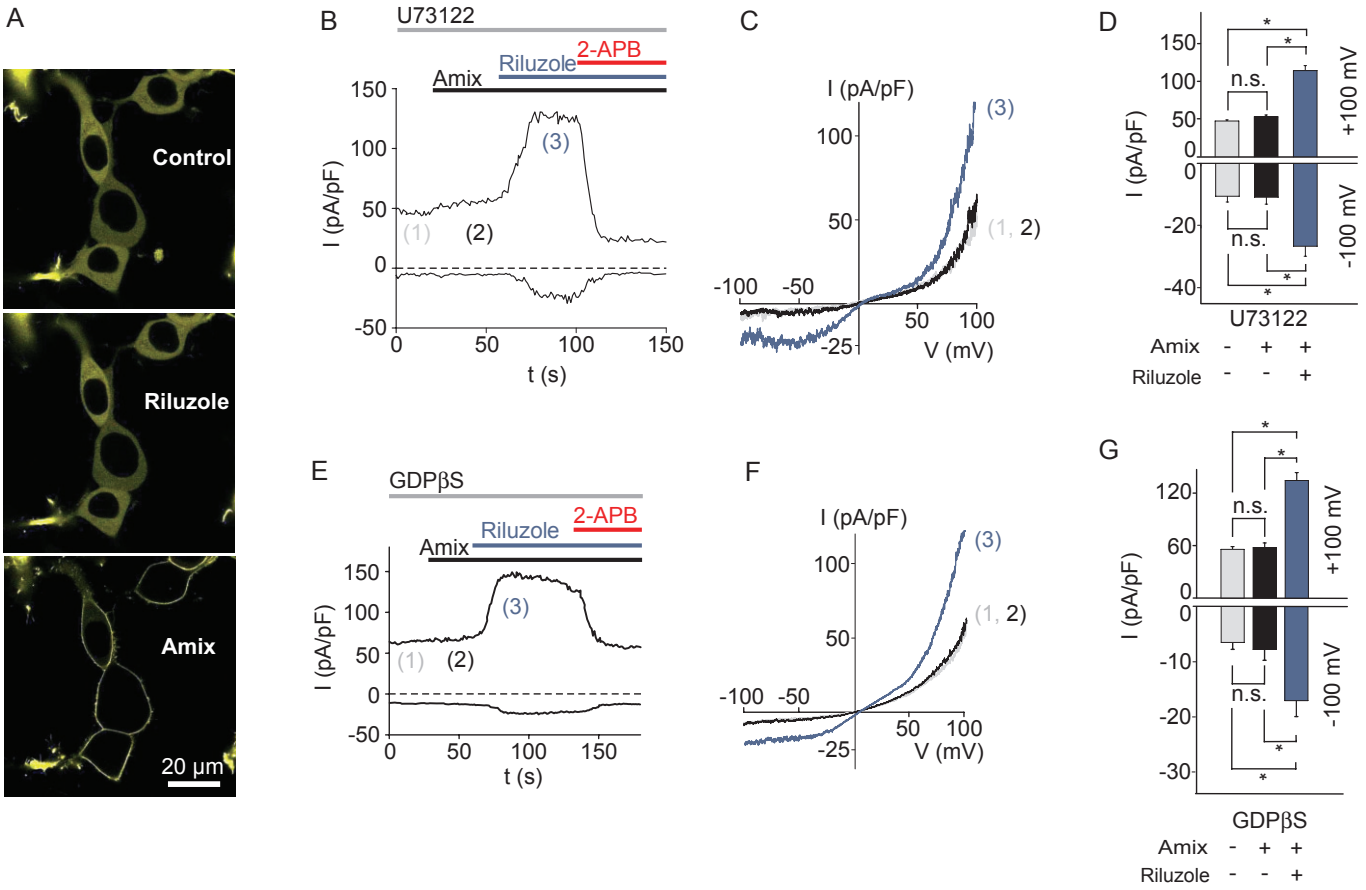

Figure 4

Riluzole-mediated TRPC5 activation is independent of G protein signalling. (A) Living HEK293 cells, stably expressing PKCε-YFP were visualized with confocal laser scanning microscopy. Subcellular localization of PKCε-YFP in untreated control cells and after addition of riluzole (50 µM) or Amix. (B) Whole-cell patch clamp recording of a T-REx$_{TRPC5}$ (Tet+) cell, pretreated with U73122 (5 µM). Data were extracted from voltage ramps and depicts current densities at +100 mV and –100 mV. Cells were exposed to Amix, riluzole (50 µM) and 2-APB (75 µM). (C) I/V curves of basal (1), Amix- (2) and riluzole- (3) induced currents. (D) Statistical analysis of nine independent experiments such as in (B). Data represent means and SEM. (E) Whole-cell recording in the presence of GDPβS (1 mM) in the patch pipette. Data were extracted from voltage ramps and depict current densities at +100 mV (upper trace) and –100 mV (lower trace) (F) I/V curves of basal (1), Amix- (2), and riluzole- (3) induced currents. (G) Statistical analysis of five independent experiments such as in (E); *$P < 0.05$, n.s., no significant difference. Data represent means and SEM.

that PLC was not strongly activated. However, PKCε efficiently translocated to the plasma membrane when stimulated with the mixture of agonists (Figure 4A). Furthermore, treatment of T-REx$_{TRPC5}$ cells with the PLC inhibitor U73122 (5 µM), which did impede TRPC5 activation by agonist mix, left riluzole-mediated TRPC5 activation unaffected (Figure 4B–D). In control experiments, using the inactive analogue of U73343 (5 µM), cells responded both to agonist mix and to riluzole addition (Supporting Information Figure S1). Although riluzole did not affect PLC activity, we conducted further experiments to rule out an involvement of other components upstream of PLC activity. To inhibit G protein activation, we intracellularly perfused T-REx$_{TRPC5}$ cells with 1 mM GDPβS, a non-hydrolysable GDP analogue. Subsequent whole-cell patch clamp recordings revealed that GDPβS prevented the agonist mix-induced TRPC5 activation, while riluzole was still effective in activating robust TRPC5 currents in the presence of intracellular GDPβS (Figure 4E–G).

Riluzole activates TRPC5 channels in inside-out and cell attached patches

To examine whether soluble intracellular components are necessary for the riluzole-mediated TRPC5 activation, we analysed the activation of TRPC5 channels in excised inside-out patches. Application of 100 µM riluzole to the cytosolic side of the channel induced a robust TRPC5 activation, which was evident as a strong increase in the open probability of the channels, as represented by the NPo (Figure 5A, B). Riluzole-induced single-channel currents recorded at different voltages displayed the typical outwardly rectifying conductance and a reversal potential close to 0 mV (Figure 5C). The average single-channel conductance at a membrane potential of –80 mV was 53 ± 2 pS (n = 6), which is in line with previously reported values for TRPC5 conductances, ranging from 38 to 63 pS (Schaefer *et al.*, 2000; Yamada *et al.*, 2000). Non-induced T-REx$_{TRPC5}$ (Tet-) were used as controls and did

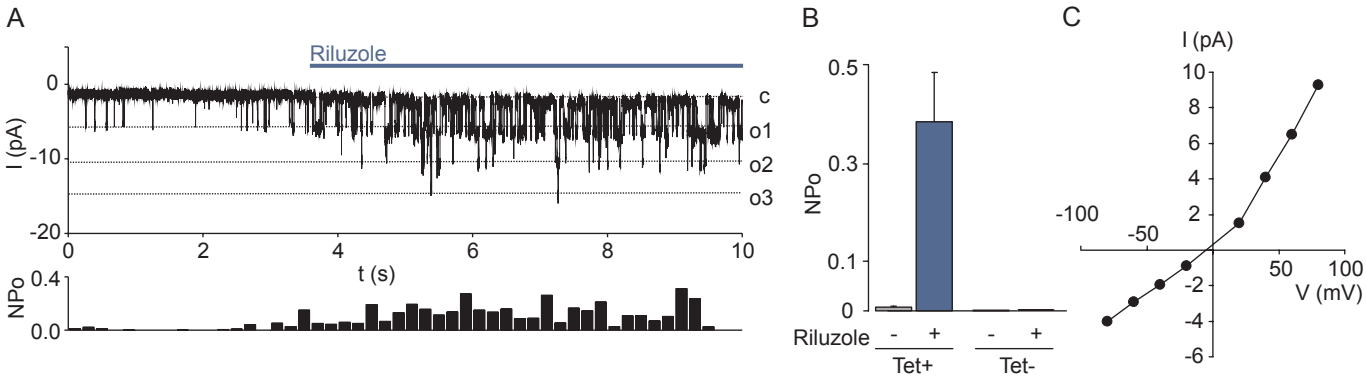

Figure 5

Riluzole activates TRPC5 channels in excised inside out patches. (A) Example trace of an inside-out patch containing at least three TRPC5 channels as indicated by the open levels (o1-o3) at −80 mV. Channel openings are downward deflections of the current trace (c). Riluzole (100 μM) was added to the bath solution as indicated by the blue bar. The NPo for the channels of the same recording was averaged over 200 ms intervals and is depicted below. (B) Statistical analysis of several independent recordings performed as shown in (A) for tet-induced cells (Tet +; n = 5) and non-induced control cells (Tet-; n = 7). The NPo was averaged for 30 s intervals before and after riluzole addition. (C) I-V curve of unitary current amplitudes recorded at different voltages.

not show any riluzole-induced channel activity (n = 7; Figure 5B). Riluzole did also evoke channel openings in 12 out of 14 cell-attached patches from induced T-REx$_{TRPC5}$ cells, when applied from the extracellular site via the patch pipette. In the presence of 2-APB (75 μM), the riluzole-induced NPo was strongly decreased (Supporting Information Figure S2).

Riluzole-induced TRPC5 activation differs from lanthanide-mediated effects

TRPC5 currents are potentiated by trivalent cations like La^{3+} and Gd^{3+} in the micromolar range. To test whether this also applies to the riluzole-activated mode of TRPC5, cells were additionally exposed to 100 μM $LaCl_3$ after riluzole treatment. Whole-cell patch clamp recordings demonstrated that La^{3+} could in fact potentiate riluzole-induced TRPC5 inward currents, even in the presence of a saturating concentration of riluzole (100 μM) by increasing the inward current amplitude from −41.8 ± 5.3 pA/pF to −72.5 ± 9.8 pA/pF (n = 7, P < 0.05; Figure 6A–C). To validate the hypothesis that riluzole acts mechanistically different from La^{3+}, we analysed TRPC5 mutants lacking the La^{3+}-induced potentiation of the current. To this end, HEK293 cells were transiently transfected with plasmids encoding point-mutated TRPC5-E543Q or TRPC5-E595Q/E598Q constructs (Jung *et al.*, 2003). As expected, electrophysiological recordings confirmed that neutralization of the negatively charged glutamate residues, located at the extracellular site near the pore mouth, resulted in the loss of potentiation by La^{3+} (Jung *et al.*, 2003). However, riluzole still induced robust currents in cells expressing the point-mutated TRPC5 channels. The amplitudes were comparable to the riluzole-induced currents measured in cell expressing the TRPC5 wild-type channel (Figure 6D).

Heteromeric TRPC1 : C5 channels are activated by riluzole

TRPC5 co-expressed with TRPC1 forms heteromeric ion channels with unique electrophysiological properties (Strubing *et al.*, 2001). To test whether this heteromer is also sensitive to riluzole, HEK293 cells were transiently transfected with expression plasmids encoding TRPC1 or TRPC5 or with a combination of both. In whole-cell patch clamp recordings, cells expressing only TRPC1 did not respond to riluzole and displayed low basal current densities of approximately 10 pA/pF at +100 mV (Figure 7A). Co-expression of TRPC1 and TRPC5, increased the basal current density to 47 ± 7.8 pA/pF (n = 4, +100 mV) and we measured a robust increase in the current densities upon riluzole treatment, which could be blocked by 2-APB (75 μM; Figure 7B). The I/V curves revealed a more outwardly rectifying current with the inward current strongly reduced compared with homomeric TRPC5 currents (Figure 7C), resembling the typical characteristics of the TRPC1 : TRPC5 heteromer (Strubing *et al.*, 2001). The riluzole-induced inward and outward current amplitudes of TRPC1 : TRPC5 were about twofold higher compared with currents stimulated with the agonist mixture alone (Figure 7D).

Riluzole activates TRPC5 endogenously expressed in the U-87 glioblastoma cell line

TRPC5 has been shown to be expressed in the glioblastoma cell line U-87 (Wang *et al.*, 2009). We, therefore, tested whether riluzole can activate native TRPC5 channels in such cells. Fura-2-based $[Ca^{2+}]_i$ measurements showed that about 71% of U-87 cells responded to riluzole treatment (100 μM) with a persistent elevation in $[Ca^{2+}]_i$, (368 ± 41 nM, n = 5; Figure 8C). The percentage of riluzole-responding cells was determined by defining a threshold of 50 nM $[Ca^{2+}]_i$ elevation compared with the resting calcium level. To clearly assign this response to TRPC5 channel activity, we treated U-87 cells with siRNA targeted against TRPC5 (si C5), which reduced TRPC5 mRNA expression (Supporting Information Figure S3). As a control, U-87 cells were treated with scrambled siRNA (si sc), which left TRPC5 mRNA expression unaffected. Both, scrambled siRNA but also TRPC5 siRNA did not alter expres-

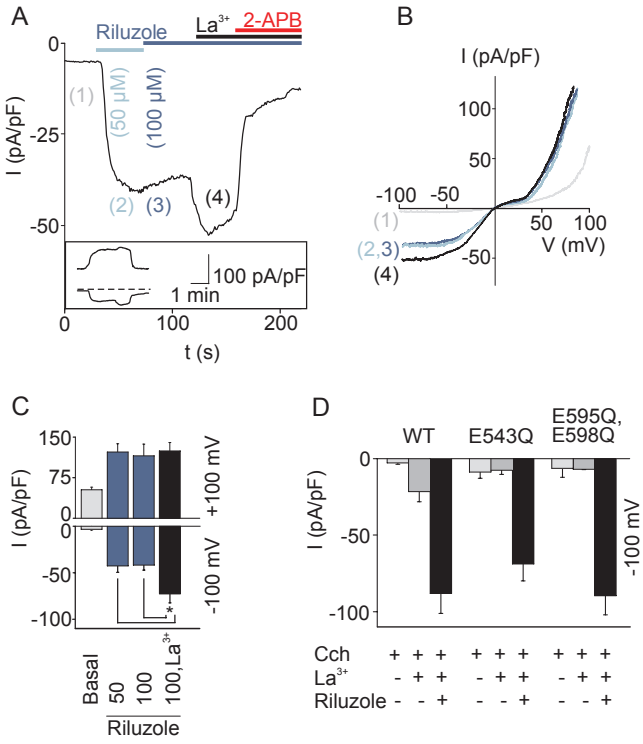

Figure 6

Riluzole-induced TRPC5 activation acts differently from the stimulating effects of lanthanum ions (La^{3+}). (A, B) Representative whole-cell recording in a T-REx$_{TRPC5}$ cell stimulated with saturating concentrations of riluzole (50, 100 µM), followed by application of 100 µM La^{3+} and 2-APB (75 µM). Data were extracted from voltage ramps and depict current densities at –100 mV. Inset: current densities at +100 mV (upper trace) and –100 mV (lower trace) at a scale of 1:3. (B) I/V curves for basal (1), 50 µM riluzole- (2), 100 µM riluzole- (3) and La^{3+}- (4) induced currents. (C) Statistical analysis as mean and SEM of five independent experiments performed as shown in (A); $^*P < 0.05$. (D) Statistical analysis of similar experiments such as in (A) but with transiently transfected HEK293 cells expressing either wild-type TRPC5 (WT) or E543Q and E595/598Q point-mutated TRPC5 constructs. Data represent peak current densities at –100 mV after treatment with carbachol (300 µM), La^{3+} (100 µM) and riluzole (50 µM) as indicated in the figure and are means and SEM of 5–7 independent experiments.

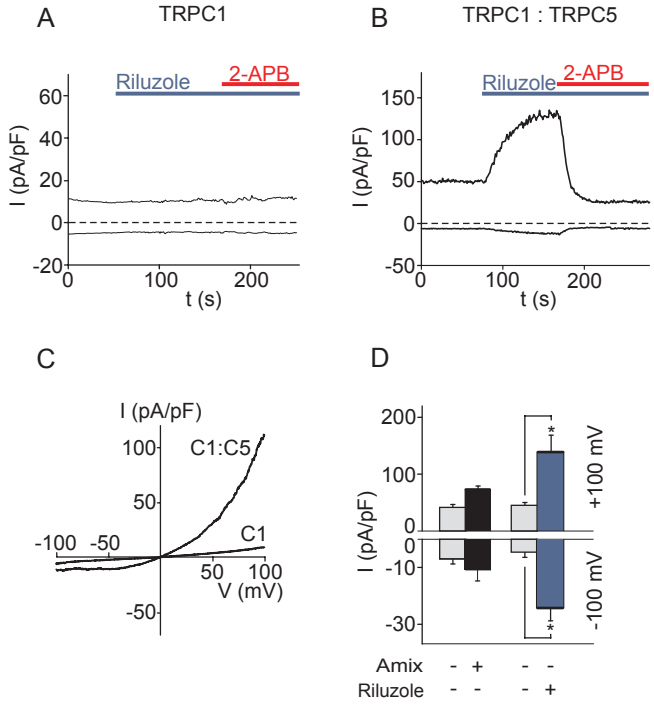

Figure 7

Riluzole activates heteromeric TRPC1: TRPC5 channels. Representative whole-cell recordings of HEK293 cells transiently transfected with expression plasmids encoding TRPC1 (A) or TRPC1 and TRPC5 in equal quantities (B). Data were extracted from voltage ramps and show current densities at +100 mV (upper trace) and –100 mV (lower trace). Channels were treated with riluzole (50 µM) and 2-APB (75 µM). (C) I/V curves for TRPC1 currents and TRPC1: TRPC5 currents after riluzole application. (D) Statistical analysis of several independent experiments such as in (B). Peak values for current densities before and after Amix addition ($n = 4$) and before and after riluzole addition (50 µM; $n = 5$; $^*P < 0.05$) are shown. Data represent means and SEM.

sion of the housekeeping gene GAPDH (Supporting Information Figure S3). Since the siRNA was not labelled, we analysed 100 randomly chosen cells per measurement. The statistical analysis of several experiments indicated that, upon si C5 treatment, the percentage of riluzole-sensitive U-87 cells decreased to 41% with an average $[Ca^{2+}]_i$ response of 203 ± 31 nM ($n = 9$, Figure 8B, C). In contrast, 79% of the control cells treated with si sc were riluzole-sensitive and responded to riluzole treatment with a mean $[Ca^{2+}]_i$ signal of 397 ± 56 nM ($n = 6$; Figure 8A, C). The riluzole-induced elevation in $[Ca^{2+}]_i$ could be blocked upon application of 2-APB (75 µM; Figure 8A, B). Electrophysiological analyses revealed that riluzole induced TRPC5-like currents in U-87 cells (Figure 8D–F), which could be blocked by high concentrations of La^{3+} (1 mM), as described before for heterologously expressed TRPC5 channels (Jung *et al.*, 2003). When permeable cations in the extracellular solution were substituted with the impermeant cation N-methyl-D-glucamine (NMDG), the inward current was eliminated, indicating that the elicited current was indeed carried by cations (Figure 8G, H).

Discussion

Riluzole is a derivative of benzothiazole that, besides its neuroprotective effect, demonstrates anti-convulsant, anti-tumour and psychotropic biological activities (Du *et al.*, 2007; Lee *et al.*, 2011). We here present riluzole as a novel activator of TRPC5 channels. It does not strongly affect either other members of the canonical TRP family, the vanilloid receptor family members TRPV1-TRPV4 or TRPM3 and TRPM8. While it seems clear that DAG, produced by PLC, directly stimulates canonical TRPC3/6/7 channels, the activation of TRPC5 still remains elusive. The Gαq–PLC pathway has been show to efficiently activate TRPC5 channels, suggesting that PLC-mediated phosphatidylinositol 4,5-bisphosphate breakdown

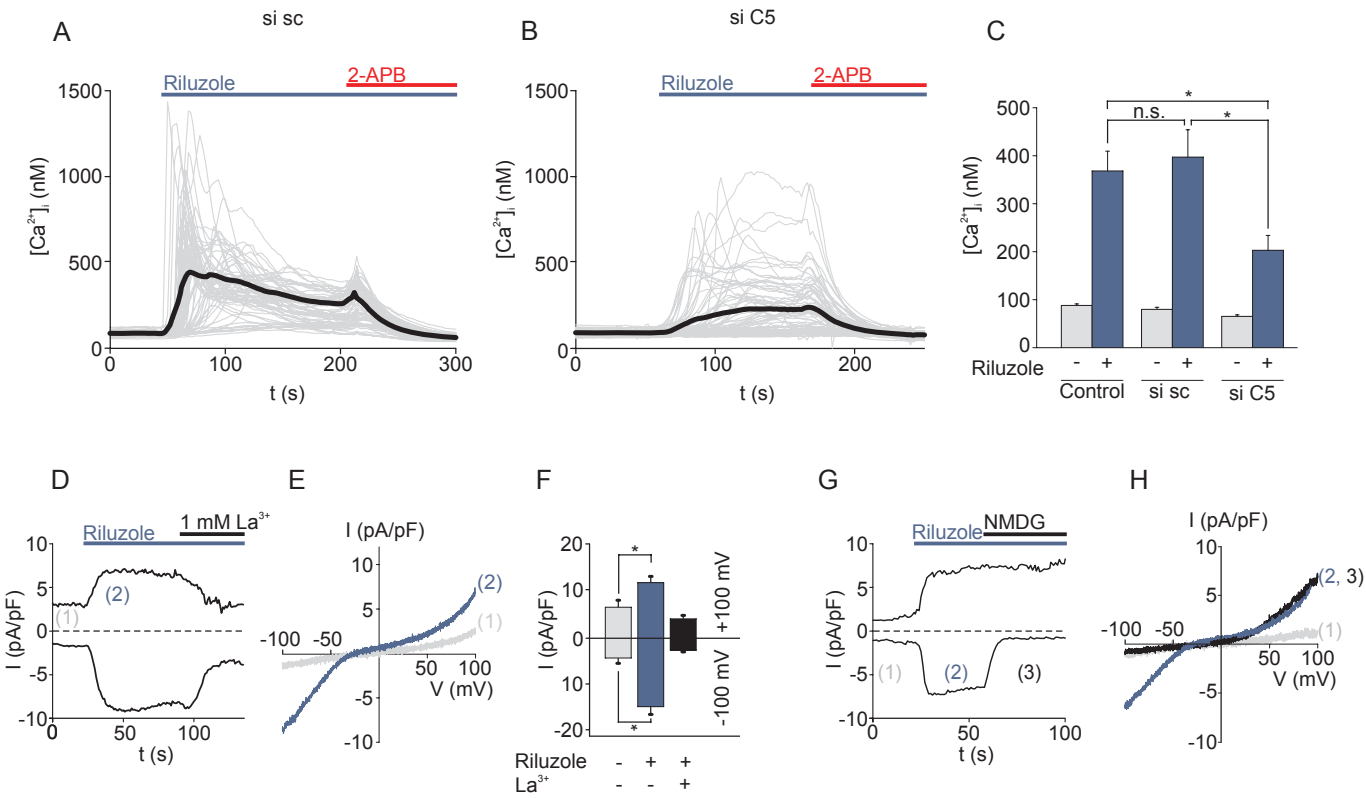

Figure 8

TRPC5 endogenously expressed in the U-87 glioblastoma cell line is activated by riluzole. (A, B) Fura-2-based $[Ca^{2+}]_i$ measurements in U-87 cells transiently transfected with 100 pmol of unspecific scrambled siRNA (si sc; A) or with TRPC5-specific siRNA (si C5; B); 72 h after transfection, time-lapse analyses of calcium signals were measured after riluzole (100 μM) application. The riluzole-induced signal was blocked by 2-APB (75 μM). (C) Statistical analysis: mean ± SEM of 5–9 independent measurements such as in (A) and (B); untreated U-87 cells served as control. For each experiment, 100 randomly chosen cells were analysed. The maximum $[Ca^{2+}]_i$ response of each cell was determined within 50 s after riluzole application (*$P < 0.05$; n.s., statistically not significant). (D) Representative whole-cell recording of a U-87 cell during addition of riluzole (100 μM) and of La^{3+} (1 mM). Data were extracted from voltage ramps and depict current densities at +100 mV (upper trace) and –100 mV (lower trace). (E) I/V curves for basal (1) and riluzole-induced (2) current. (F) Statistical analysis of several experiments such as in (D). Data represent peak current densities and are means and SEM of five independent experiments. (G) Representative whole-cell recording of a U-87 cell stimulated with riluzole (50 μM), before and after permeable cations in the bath solution were substituted with NMDG. (H) I/V curves for basal (1), riluzole-incuded currents in standard extracellular solution (2) and riluzole-induced current in 140 mM NMDG extracellular solution (3).

is involved in the cascade that results in the opening of TRPC5 channels (Clapham, 2003). In the present study, we examined whether riluzole triggers signalling events in this pathway. The inhibition of G proteins via intracellularly perfused GDPβS did not block the riluzole-mediated activation of TRPC5, indicating that G proteins are not directly involved in the activation process. Furthermore, there was neither a discernible production of DAG upon riluzole treatment of HEK293 cells nor was the riluzole-induced TRPC5 activation sensitive towards the PLC inhibitor U73122, indicating that PLC activity is not required for the action of riluzole on TRPC5. Considering also that the closely related TRPC4 channel was largely insensitive to riluzole treatment, we conclude that riluzole activates TRPC5 channels independently of the classical receptor-activated mechanism. Several factors, which lead to an increase in TRPC5 activity, have recently been identified. High intracellular calcium concentrations of up to 1 μM, for example, increase TRPC5 activity 25-fold (Blair *et al.*, 2009). We assume that changes in the intracellular calcium concentration do not underlie the riluzole-mediated activation of TRPC5, as riluzole was still effective in inside-out patches where the calcium concentration was strongly buffered and adjusted to 100 nM. Trivalent cations like La^{3+} and Gd^{3+} or divalent Pb^{2+}, and acidic extracellular pH efficiently potentiate TRPC5 independently of GPCR activation; and the amino acids involved in the binding of lanthanides and lead have already been identified (Jung *et al.*, 2003; Semtner *et al.*, 2007; Sukumar and Beech, 2010). We showed that these sites are not involved in the riluzole-mediated activation of TRPC5, indicating that the molecular mechanisms are different from those of lanthanides, Pb^{2+} and protons. TRPC5 has also been reported to be inhibited by cAMP via PKA-dependent phosphorylation (Sung *et al.* 2011). Although riluzole influences intracellular cAMP levels, presumably by inhibiting PDE (Duprat *et al.*, 2000), it seems unlikely that such a mechanism underlies the action of riluzole on TRPC5, as increased cAMP levels would more likely result in a block of TRPC5.

Another possibility for regulating the availability of functional TRPC5 channels in the plasma membrane may occur via a rapid insertion of TRPC5-containing vesicles into the plasma membrane upon stimulation of growth factor receptors (Bezzerides *et al.*, 2004). This process is regulated by PI3K, Rac1 and phosphatidylinositol 4-phosphate 5 kinase and is usually relatively slow with a latency of ~200 s. We do not think that such an externalization of TRPC5 channels underlies the riluzole-mediated activation of TRPC5 as the onset of the riluzole activation of TRPC5 in whole-cell recordings was fast and occurred within a few seconds.

The single-channel conductance after riluzole stimulation is not different from the one evoked by receptor stimulation, indicating that riluzole treatment results in an increase in the open probability of TRPC5 channels. As riluzole could activate TRPC5 currents in the excised inside-out configuration, it is clear that the action of riluzole does not require cytosolic factors, suggesting that the membrane-confining action of riluzole on TRPC5 channels is a direct effect of the compound. Although in our patch clamp studies riluzole was effective when applied from either side of the membrane, we cannot differentiate whether riluzole acts from the intra- or extracellular site due to its highly lipophilic character. Furthermore, apart from directly binding to the channel protein itself, riluzole could alternatively partition into the lipid bilayer, thereby altering the physical properties of the surrounding lipid environment, which may in turn cause the opening of TRPC5 channels, a mechanism that has been suggested for the effects of lysoPC and of volatile anaesthetics on TRPC5 channels (Flemming *et al.*, 2006; Bahnasi *et al.*, 2008).

The endogenous expression of TRPC5 and TRPC1 shows an overlapping pattern as TRPC1:TRPC5 can form heteromeric complexes (Strubing *et al.*, 2001; Zimmermann *et al.*, 2011). In line with previous reports (Strubing *et al.*, 2001; Storch *et al.*, 2012), overexpressed TRPC1 did not show any basal or receptor-activated conductance in our hands, nor was it affected by riluzole treatment, whereas TRPC1 : TRPC5 heteromers could be efficiently activated by riluzole in a similar manner to the homomer.

The presence of TRPC5 transcripts has been detected in several cancer cell lines, including the adriamycin-resistant MCF-7 breast cancer cell line (Ma *et al.*, 2012) and the glioblastoma/astrocytomas cell line U-87 (Wang *et al.*, 2009). We were able to induce a riluzole-mediated calcium entry in U-87 cells, which was decreased after siRNA-mediated knockdown of TRPC5. Moreover, riluzole also evoked TRPC5-like currents in whole-cell patch clamp recordings on U-87 cells, indicating that endogenous TRPC5 channels can be activated by riluzole.

At present, it is not clear whether the effect of riluzole on TRPC5 is clinically relevant. The plasma concentration in ALS patients receiving treatment with riluzole at typical doses of 100 mg·day^{-1} is about 2 μM (Mohammadi *et al.*, 2002). At this concentration, only minor effects of riluzole on TRPC5 channels may be expected. However, according to animal studies, the concentration of riluzole in the brain is thought to be fivefold higher compared with the plasma levels (Colovic *et al.*, 2004; Cheah *et al.*, 2010). As we have shown that riluzole at a concentration of 10 μM is sufficient to strongly potentiate receptor-activated TRPC5 currents in patch clamp studies, it may be possible that some of the reported physiological effects and side effects of riluzole *in vivo* may be caused by the activation of homomeric TRPC5 or heteromeric TRPC1 : TRPC5 channels.

Acknowledgements

The HEK cell line, stably expressing a myc-tagged mouse TRPM3α2 construct, was a kind gift from Stephan Philipp (Universitaet des Saarlandes, Homburg, Germany). The authors thank Nicole Urban, Marion Leonhardt and Helga Sobottka for their excellent technical assistance. This work was supported by the Deutsche Forschungsgemeinschaft (HI 829/2-1 to K. H.).

Conflict of interest

The authors state no conflict of interest.

References

Alexander SPH *et al.* (2013). The Concise Guide to PHARMACOLOGY 2013/14: Overview. Br J Pharmacol 170: 1449–1867.

Bahnasi YM, Wright HM, Milligan CJ, Dedman AM, Zeng F, Hopkins PM *et al.* (2008). Modulation of TRPC5 cation channels by halothane, chloroform and propofol. Br J Pharmacol 153: 1505–1512.

Beech DJ, Muraki K, Flemming R (2004). Non-selective cationic channels of smooth muscle and the mammalian homologues of Drosophila TRP. J Physiol 559: 685–706.

Bellingham MC (2011). A review of the neural mechanisms of action and clinical efficiency of riluzole in treating amyotrophic lateral sclerosis: what have we learned in the last decade? CNS Neurosci Ther 17: 4–31.

Bezzerides VJ, Ramsey IS, Kotecha S, Greka A, Clapham DE (2004). Rapid vesicular translocation and insertion of TRP channels. Nat Cell Biol 6: 709–720.

Blair NT, Kaczmarek JS, Clapham DE (2009). Intracellular calcium strongly potentiates agonist-activated TRPC5 channels. J Gen Physiol 133: 525–546.

Cheah BC, Vucic S, Krishnan AV, Kiernan MC (2010). Riluzole, neuroprotection and amyotrophic lateral sclerosis. Curr Med Chem 17: 1942–1959.

Clapham DE (2003). TRP channels as cellular sensors. Nature 426: 517–524.

Colovic M, Zennaro E, Caccia S (2004). Liquid chromatographic assay for riluzole in mouse plasma and central nervous system tissues. J Chromatogr B Analyt Technol Biomed Life Sci 803: 305–309.

Du J, Suzuki K, Wei Y, Wang Y, Blumenthal R, Chen Z *et al.* (2007). The anticonvulsants lamotrigine, riluzole, and valproate differentially regulate AMPA receptor membrane localization:

relationship to clinical effects in mood disorders. Neuropsychopharmacology 32: 793–802.

Duprat F, Lesage F, Patel AJ, Fink M, Romey G, Lazdunski M (2000). The neuroprotective agent riluzole activates the two P domain K(+) channels TREK-1 and TRAAK. Mol Pharmacol 57: 906–912.

Flemming PK, Dedman AM, Xu SZ, Li J, Zeng F, Naylor J *et al.* (2006). Sensing of lysophospholipids by TRPC5 calcium channel. J Biol Chem 281: 4977–4982.

Fowler MA, Sidiropoulou K, Ozkan ED, Phillips CW, Cooper DC (2007). Corticolimbic expression of TRPC4 and TRPC5 channels in the rodent brain. PLoS ONE 2: e573.

Fruhwald J, Camacho LJ, Dembla S, Mannebach S, Lis A, Drews A *et al.* (2012). Alternative splicing of a protein domain indispensable for function of transient receptor potential melastatin 3 (TRPM3) ion channels. J Biol Chem 287: 36663–36672.

Goel M, Sinkins WG, Schilling WP (2002). Selective association of TRPC channel subunits in rat brain synaptosomes. J Biol Chem 277: 48303–48310.

Grant P, Song JY, Swedo SE (2010). Review of the use of the glutamate antagonist riluzole in psychiatric disorders and a description of recent use in childhood obsessive-compulsive disorder. J Child Adolesc Psychopharmacol 20: 309–315.

Greka A, Navarro B, Oancea E, Duggan A, Clapham DE (2003). TRPC5 is a regulator of hippocampal neurite length and growth cone morphology. Nat Neurosci 6: 837–845.

Hofmann T, Schaefer M, Schultz G, Gudermann T (2002). Subunit composition of mammalian transient receptor potential channels in living cells. Proc Natl Acad Sci U S A 99: 7461–7466.

Huang CS, Song JH, Nagata K, Yeh JZ, Narahashi T (1997). Effects of the neuroprotective agent riluzole on the high voltage-activated calcium channels of rat dorsal root ganglion neurons. J Pharmacol Exp Ther 282: 1280–1290.

Hui H, McHugh D, Hannan M, Zeng F, Xu SZ, Khan SU *et al.* (2006). Calcium-sensing mechanism in TRPC5 channels contributing to retardation of neurite outgrowth. J Physiol 572: 165–172.

Jung S, Muhle A, Schaefer M, Strotmann R, Schultz G, Plant TD (2003). Lanthanides potentiate TRPC5 currents by an action at extracellular sites close to the pore mouth. J Biol Chem 278: 3562–3571.

Kawabata A, Saifeddine M, Al-Ani B, Hollenberg MD (1997). Protease-activated receptors: development of agonists selective for receptors triggered by either thrombin (PAR1) or trypsin (PAR2). Proc West Pharmacol Soc 40: 49–51.

Lacomblez L, Bensimon G, Leigh PN, Guillet P, Powe L, Durrleman S *et al.* (1996). A confirmatory dose-ranging study of riluzole in ALS. ALS/Riluzole Study Group-II. Neurology 47: S242–S250.

Lee HJ, Wall BA, Wangari-Talbot J, Shin SS, Rosenberg S, Chan JL *et al.* (2011). Glutamatergic pathway targeting in melanoma: single-agent and combinatorial therapies. Clin Cancer Res 17: 7080–7092.

Lein ES, Hawrylycz MJ, Ao N, Ayres M, Bensinger A, Bernard A *et al.* (2007). Genome-wide atlas of gene expression in the adult mouse brain. Nature 445: 168–176.

Lenz JC, Reusch HP, Albrecht N, Schultz G, Schaefer M (2002). Ca^{2+}-controlled competitive diacylglycerol binding of protein kinase C isoenzymes in living cells. J Cell Biol 159: 291–302.

Ma X, Cai Y, He D, Zou C, Zhang P, Lo CY *et al.* (2012). Transient receptor potential channel TRPC5 is essential for P-glycoprotein induction in drug-resistant cancer cells. Proc Natl Acad Sci U S A 109: 16282–16287.

Majeed Y, Bahnasi Y, Seymour VA, Wilson LA, Milligan CJ, Agarwal AK *et al.* (2011). Rapid and contrasting effects of rosiglitazone on transient receptor potential TRPM3 and TRPC5 channels. Mol Pharmacol 79: 1023–1030.

Mohammadi B, Lang N, Dengler R, Bufler J (2002). Interaction of high concentrations of riluzole with recombinant skeletal muscle sodium channels and adult-type nicotinic receptor channels. Muscle Nerve 26: 539–545.

Munsch T, Freichel M, Flockerzi V, Pape HC (2003). Contribution of transient receptor potential channels to the control of GABA release from dendrites. Proc Natl Acad Sci U S A 100: 16065–16070.

Norenberg W, Sobottka H, Hempel C, Plotz T, Fischer W, Schmalzing G *et al.* (2012). Positive allosteric modulation by ivermectin of human but not murine P2X7 receptors. Br J Pharmacol 167: 48–66.

Otsuguro K, Tang J, Tang Y, Xiao R, Freichel M, Tsvilovskyy V *et al.* (2008). Isoform-specific inhibition of TRPC4 channel by phosphatidylinositol 4,5-bisphosphate. J Biol Chem 283: 10026–10036.

Pittenger C, Coric V, Banasr M, Bloch M, Krystal JH, Sanacora G (2008). Riluzole in the treatment of mood and anxiety disorders. CNS Drugs 22: 761–786.

Putney JW, Jr (2004). The enigmatic TRPCs: multifunctional cation channels. Trends Cell Biol 14: 282–286.

Riccio A, Medhurst AD, Mattei C, Kelsell RE, Calver AR, Randall AD *et al.* (2002). mRNA distribution analysis of human TRPC family in CNS and peripheral tissues. Brain Res Mol Brain Res 109: 95–104.

Riccio A, Li Y, Moon J, Kim KS, Smith KS, Rudolph U *et al.* (2009). Essential role for TRPC5 in amygdala function and fear-related behavior. Cell 137: 761–772.

Schachter JB, Sromek SM, Nicholas RA, Harden TK (1997). HEK293 human embryonic kidney cells endogenously express the P2Y1 and P2Y2 receptors. Neuropharmacology 36: 1181–1187.

Schaefer M, Plant TD, Obukhov AG, Hofmann T, Gudermann T, Schultz G (2000). Receptor-mediated regulation of the nonselective cation channels TRPC4 and TRPC5. J Biol Chem 275: 17517–17526.

Schaefer M, Albrecht N, Hofmann T, Gudermann T, Schultz G (2001). Diffusion-limited translocation mechanism of protein kinase C isotypes. FASEB J 15: 1634–1636.

Schuster JE, Fu R, Siddique T, Heckman CJ (2012). Effect of prolonged riluzole exposure on cultured motoneurons in a mouse model of ALS. J Neurophysiol 107: 484–492.

Semtner M, Schaefer M, Pinkenburg O, Plant TD (2007). Potentiation of TRPC5 by protons. J Biol Chem 282: 33868–33878.

Song JH, Huang CS, Nagata K, Yeh JZ, Narahashi T (1997). Differential action of riluzole on tetrodotoxin-sensitive and tetrodotoxin-resistant sodium channels. J Pharmacol Exp Ther 282: 707–714.

Storch U, Forst AL, Philipp M, Gudermann T, Schnitzler M (2012). Transient receptor potential channel 1 (TRPC1) reduces calcium permeability in heteromeric channel complexes. J Biol Chem 287: 3530–3540.

Strubing C, Krapivinsky G, Krapivinsky L, Clapham DE (2001). TRPC1 and TRPC5 form a novel cation channel in mammalian brain. Neuron 29: 645–655.

Strubing C, Krapivinsky G, Krapivinsky L, Clapham DE (2003). Formation of novel TRPC channels by complex subunit interactions in embryonic brain. J Biol Chem 278: 39014–39019.

Sukumar P, Beech DJ (2010). Stimulation of TRPC5 cationic channels by low micromolar concentrations of lead ions (Pb^{2}+). Biochem Biophys Res Commun 393: 50–54.

Sung TS, Jeon JP, Kim BJ, Hong C, Kim SY, Kim J *et al*. (2011). Molecular determinants of PKA-dependent inhibition of TRPC5 channel. Am J Physiol Cell Physiol 301: 823–832.

Thyagarajan B, Benn BS, Christakos S, Rohacs T (2009). Phospholipase C-mediated regulation of transient receptor potential vanilloid 6 channels: implications in active intestinal Ca^{2+} transport. Mol Pharmacol 75: 608–616.

Urban N, Hill K, Wang L, Kuebler WM, Schaefer M (2012). Novel pharmacological TRPC inhibitors block hypoxia-induced vasoconstriction. Cell Calcium 51: 194–206.

Wang B, Li W, Meng X, Zou F (2009). Hypoxia up-regulates vascular endothelial growth factor in U-87 MG cells: involvement of TRPC1. Neurosci Lett 459: 132–136.

Wang YJ, Lin MW, Lin AA, Wu SN (2008). Riluzole-induced block of voltage-gated Na^{+} current and activation of BKCa channels in cultured differentiated human skeletal muscle cells. Life Sci 82: 11–20.

Wong CO, Huang Y, Yao X (2010). Genistein potentiates activity of the cation channel TRPC5 independently of tyrosine kinases. Br J Pharmacol 159: 1486–1496.

Wu G, Lu ZH, Obukhov AG, Nowycky MC, Ledeen RW (2007). Induction of calcium influx through TRPC5 channels by cross-linking of GM1 ganglioside associated with alpha5beta1 integrin initiates neurite outgrowth. J Neurosci 27: 7447–7458.

Wu SN, Li HF (1999). Characterization of riluzole-induced stimulation of large-conductance calcium-activated potassium channels in rat pituitary GH3 cells. J Investig Med 47: 484–495.

Xu SZ, Zeng F, Boulay G, Grimm C, Harteneck C, Beech DJ (2005). Block of TRPC5 channels by 2-aminoethoxydiphenyl borate: a differential, extracellular and voltage-dependent effect. Br J Pharmacol 145: 405–414.

Yamada H, Wakamori M, Hara Y, Takahashi Y, Konishi K, Imoto K *et al*. (2000). Spontaneous single-channel activity of neuronal TRP5 channel recombinantly expressed in HEK293 cells. Neurosci Lett 285: 111–114.

Zhu X, Jiang M, Birnbaumer L (1998). Receptor-activated Ca^{2+} influx via human Trp3 stably expressed in human embryonic kidney (HEK)293 cells. Evidence for a non-capacitative Ca^{2+} entry. J Biol Chem 273: 133–142.

Zimmermann K, Lennerz JK, Hein A, Link AS, Kaczmarek JS, Delling M *et al*. (2011). Transient receptor potential cation channel, subfamily C, member 5 (TRPC5) is a cold-transducer in the peripheral nervous system. Proc Natl Acad Sci U S A 108: 18114–18119.

Supporting information

Additional Supporting Information may be found in the online version of this article at the publisher's web-site:

http://dx.doi.org/10.1111/bph.12436

Figure S1 U73343, the inactive analogue of U73122, does not interfere with the riluzole-mediated TRPC5 activation. Whole cell patch clamp recording of T-REx$_{TRPC5}$ (Tet+) cells pretreated with U73343 (5 μM). (A) Representative whole cell recording. Data were extracted from voltage ramps and represent current densities at +100 mV (upper trace) and –100 mV (lower trace) in response to Amix, riluzole (50 μM), and 2-APB (75 μM). (B) I/V curves for basal (1), Amix (2)-, and riluzole (3)-induced currents. (C) Statistical analysis of several experiments such as in A (*P < 0.05, n.s.: no significant difference). Data represent means and SEM of 5 independent experiments.

Figure S2 Riluzole activates TRPC5 in cell-attached patches. Examples of cell-attached recordings on tetracycline induced T-REx$_{TRPC5}$ (Tet+; upper trace) and non-induced T-REx$_{TRPC5}$ (Tet-; lower trace) cells at –80 mV. Pipette and bath solution consist of standard extracellular buffer, the pipette solution was additionally supplemented with 100 μM riluzole or with 100 μM riluzole together with 75 μM 2-APB as indicated. (Right-hand figure) The NPo was averaged for 30s intervals and represent means and SEM of several independent experiments. Numbers of individual experiments are stated in the figure.

Figure S3 Gene expression of TRPC1, TRPC5 and GAPDH in U87 cells, which were transiently transfected with TRPC5-specific siRNA (100 pmol, si C5) or unspecific scrambled siRNA (100 pmol, si sc). Untreated U87 cells served as a control. Total RNA was isolated by using RNeasy Mini Kit purchased from Qiagen. The RNA (1 μg) was reverse transcribed to obtain cDNA by using M-MuLV Reverse Transcriptase according to the manufacturer's instructions (NEB: Ipswich, MA, USA). The PCRs were carried out on PTC-200 DNA Engine Cycler (Bio-Rad: Hercules, CA, USA) by using GoTaq DNA Polymerase Kit obtained from Promega (Madison, WI, USA). The following primers were used: TRPC1 forward primer: AGTGACGAGCCTCTTGACAAAC, reverse primer: GGGCTTGCGTCGGTAAC. TRPC5 forward primer: AACTCCCTCTACCTGGCAACTA, reverse primer: GGATATG AGACGCAACGAACTT. GAPDH forward primer: CTCATTT CCTGGTATGAC, reverse primer: GAGCACAGGGTACTTTAT. The cDNA was amplified for 35 cycles (TRPC1, TRPC5) or 22 cycles (GAPDH) and PCR products (5 μL) were subjected to 1% agarose gel electrophoresis.